

ORIGINAL PAPER

XPO1 mutations identify early-stage CLL characterized by shorter time to first treatment and enhanced BCR signalling

Riccardo Moia¹  | Lodovico Terzi di Bergamo^{2,3,4} | Donatella Talotta¹ | Riccardo Bomben⁵  |
 Gabriela Forestieri² | Valeria Spina² | Alessio Bruscatelli² | Chiara Cosentino¹ |
 Mohammad Almasri¹ | Riccardo Dondolin¹ | Tamara Bittolo⁵ | Antonella Zucchetto⁵ |
 Stefano Baldoni⁶ | Ilaria Del Giudice⁷  | Francesca Romana Mauro⁷  |
 Rossana Maffei⁸  | Annalisa Chiarenza⁹ | Agostino Tafuri¹⁰ | Roberta Laureana¹¹ |
 Maria Ilaria Del Principe¹¹ | Francesco Zaja¹² | Giovanni D'Arena¹³  | Jacopo Olivieri¹⁴ |
 Silvia Rasi¹ | Abdurraouf Mahmoud¹ | Wael Al Essa¹ | Bassel Awikeh¹ |
 Sreekar Kogila¹ | Matteo Bellia¹ | Samir Mouhssine¹ | Paolo Sportoletti⁶  |
 Roberto Marasca⁸ | Lydia Scarfò¹⁵  | Paolo Ghia¹⁵  | Valter Gattei⁵ | Robin Foà⁷  |
 Davide Rossi² | Gianluca Gaidano¹ 

¹Division of Hematology, Department of Translational Medicine, Università del Piemonte Orientale, Novara, Italy

²Laboratory of Experimental Hematology, Institute of Oncology Research, Bellinzona, Switzerland

³Bioinformatics Core Unit, Swiss Institute of Bioinformatics, Bellinzona, Switzerland

⁴Department of Health Science and Technology, Swiss Federal Institute of Technology (ETH Zürich), Zurich, Switzerland

⁵Clinical and Experimental Onco-Hematology Unit, Centro di Riferimento Oncologico di Aviano (CRO), IRCCS, Aviano, Italy

⁶Institute of Hematology, Center for Hemato-Oncology Research, Santa Maria della Misericordia Hospital, University of Perugia, Perugia, Italy

⁷Hematology, Department of Translational and Precision Medicine, 'Sapienza' University, Rome, Italy

⁸Section of Hematology, Department of Medical Sciences, University of Modena and Reggio Emilia, Modena, Italy

⁹A.O.O. Policlinico "G. Rodolico-S. Marco", U.O.C. Ematologia, Catania, Italy

¹⁰Department of Clinical and Molecular Medicine, Hematology Sant'Andrea University Hospital, Sapienza University of Rome, Rome, Italy

¹¹Division of Hematology, University of Tor Vergata, Rome, Italy

¹²SC Ematologia, Azienda Sanitaria Universitaria Integrata, Trieste, Italy

¹³Ematologia, P.O. San Luca, ASL Salerno, Vallo della Lucania, Italy

¹⁴Azienda Sanitaria Universitaria Friuli Centrale (ASU FC), SOC Clinica Ematologica, Udine, Italy

¹⁵IRCCS Ospedale San Raffaele, Università Vita Salute San Raffaele, Milan, Italy

Correspondence

Riccardo Moia, Division of Hematology,
 Department of Translational Medicine,
 University of Eastern Piedmont, Via Solaroli
 17, 28100 Novara, Italy.
 Email: riccardo.moia@uniupo.it

Funding information

Associazione Italiana per la Ricerca sul
 Cancro, Grant/Award Number: 21198;
 Ministero della Salute, Grant/Award Number:
 RF-2018-12365790; Ministero dell'Istruzione,

Summary

Here we evaluated the epigenomic and transcriptomic profile of *XPO1* mutant chronic lymphocytic leukaemia (CLL) and their clinical phenotype. By ATAC-seq, chromatin regions that were more accessible in *XPO1* mutated CLL were enriched of binding sites for transcription factors regulated by pathways emanating from the B-cell receptor (BCR), including NF- κ B signalling, p38-JNK and RAS-RAF-MEK-ERK. *XPO1* mutant CLL, consistent with the chromatin accessibility changes, were enriched with transcriptomic features associated with BCR and cytokine signalling.

Davide Rossi and Gianluca Gaidano equally contributed to this work.

[Corrections made on 4 October 2023, after first online publication: The 2nd author's name was corrected and ORCID was added to Gianluca Gaidano in this version.]

This is an open access article under the terms of the [Creative Commons Attribution-NonCommercial-NoDerivs](https://creativecommons.org/licenses/by-nc-nd/4.0/) License, which permits use and distribution in any medium, provided the original work is properly cited, the use is non-commercial and no modifications or adaptations are made.

© 2023 The Authors. *British Journal of Haematology* published by British Society for Haematology and John Wiley & Sons Ltd.

dell'Università e della Ricerca, Grant/Award Number: PRIN; 2015ZMRFEA; Swiss Cancer League, Grant/Award Number: 3746, 4395, 4660 and 4705; Swiss National Science Foundation, Grant/Award Number: 320030_169670/1 and 310030_192439; The Leukemia & Lymphoma Society, Translational Research Program, Grant/Award Number: 6594-20

By combining epigenomic and transcriptomic data, *MIR155HG*, the host gene of miR-155, and *MYB*, the transcription factor that positively regulates *MIR155HG*, were upregulated by RNA-seq and their promoters were more accessible by ATAC-seq. To evaluate the clinical impact of *XPO1* mutations, we investigated a total of 957 early-stage CLL subdivided into 3 independent cohorts ($N=276$, $N=286$ and $N=395$). Next-generation sequencing analysis identified *XPO1* mutations as a novel predictor of shorter time to first treatment (TTFT) in all cohorts. Notably, *XPO1* mutations maintained their prognostic value independent of the immunoglobulin heavy chain variable status and early-stage prognostic models. These data suggest that *XPO1* mutations, conceivably through increased miR-155 levels, may enhance BCR signalling leading to higher proliferation and shorter TTFT in early-stage CLL.

KEYWORDS
 BCR, CLL, *XPO1*

INTRODUCTION

Genomic analysis of chronic lymphocytic leukaemia (CLL) has clarified the disease molecular landscape and has identified a panel of driver genes that includes *XPO1*.^{1–3} *XPO1* codes for exportin-1, which is one of the most important human shuttle proteins regulating the traffic of macromolecules between nucleus and cytoplasm, and is essential for cellular homeostasis.⁴ *XPO1* binds to a diverse array of proteins through their canonical leucine-rich nuclear export signal (NES) domain that serves as a consensus sequence for nuclear export.⁴ *XPO1*, in addition to CLL, is mutated in several other haematological and solid tumours.⁴ Most *XPO1* mutations detected in human cancer consist of the E571K substitution that confers a gain-of-function. In cells harbouring *XPO1*^{E571K} mutations, a negatively charged glutamic acid at position E571 is substituted with a positively charged lysine. This change enhances interaction of *XPO1*^{E571K} with proteins bearing negatively charged NES sequences thus translating into an augmented export of negatively charged cargo proteins.⁵

The B-cell receptor (BCR) signalling is essential for CLL pathogenesis and proliferation.^{6,7} Compared to normal B cells, the BCR of many CLL cells is characterized by an intrinsically higher reactivity to antigens.^{6,7} In cases of unmutated immunoglobulin heavy chain variable (IGHV) rearrangements and in the presence of specific stereotyped BCR (e.g. subset #2), BCR activation is also enhanced in an antigen-independent manner driven by homotypic BCR to BCR interactions.^{8,9} Few data are reported about the interplay between specific gene mutations and BCR activity.

Most of newly diagnosed CLL patients with CLL do not require therapy initially, as they present a lymphocytosis but do not have any additional symptoms or complete blood count abnormalities, and do not have enlarged lymph nodes or splenomegaly.¹⁰ These asymptomatic patients, namely Binet A and Rai 0 CLL, are managed with a watch-and-wait strategy since early intervention with chemoimmunotherapy and/or pathway inhibitors did not show a survival benefit.^{10–14} Since most patients do not require

therapy at the time of the diagnosis, CLL provides an informative model to evaluate the disease's intrinsic mechanisms of clonal expansion without the external stimuli imposed by therapy.^{15–17} Two different prognostic models in early-stage CLL patients identified simple biological and clinical variables that clearly segregate patients who require treatment soon after the diagnosis and patients with a high probability to remain asymptomatic for decades.^{18,19} Since CLL is characterized by a high grade of molecular heterogeneity, the analysis of gene mutations may further improve the stratification of time to first treatment (TTFT) in asymptomatic CLL patients.²⁰

The aims of the present study were (i) to evaluate the prevalence of *XPO1* mutations in different phases of the CLL clinical course; (ii) to characterize the epigenomic and transcriptomic profile of *XPO1* mutant versus *XPO1* wild-type CLL and (iii) to evaluate whether *XPO1* mutations may predispose to disease progression and early treatment requirement.

MATERIALS AND METHODS

Patients and *XPO1* analysis

To evaluate the prevalence of *XPO1* mutations in different phases of the disease, we screened for *XPO1* mutations 95 monoclonal B-cell lymphocytosis (MBL), 957 early stage CLL (Rai 0/I or Binet A), 81 CLL relapsed after chemoimmunotherapy or pathway inhibitors, and 55 CLL transformed into an aggressive lymphoma (Richter syndrome). The clinical correlation between *XPO1* mutations and TTFT was analysed in 276 consecutive newly diagnosed Rai 0 and I CLL patients referring to our institution (1st cohort). The 2nd cohort was represented by a multicentre cohort of 286 Binet A CLL and the 3rd cohort by a multicentre cohort of 395 Rai 0 CLL previously described elsewhere.¹⁹ To evaluate the potential clonal evolution of *XPO1* mutations, we re-analysed patients followed at our institution at the time of treatment requirement ($N=61$) and at the time of Richter

transformation ($N=29$). We also analysed the *XPO1* gene in 33 CLL cases during ibrutinib therapy at homogeneous time points every 24 weeks for at least 96 weeks. The study was approved by the local ethical committee (study number CE 120/19).

The *XPO1* gene (exons 15 and 16) was analysed by next-generation sequencing using a targeted resequencing gene panel including the coding exons plus splice sites of 10 CLL driver genes (size of the target region: 26680 bp) in the 1st and the 3rd cohorts (Table S1). In the 2nd cohort, the *XPO1* gene was analysed by Sanger sequencing (Supplementary Appendix and Table S2). Multiplexed libraries ($n=10$ per run) were sequenced on Illumina MiSeq platform. The variant allele frequency (VAF) threshold was 5%. A robust and previously validated bioinformatics pipeline was used for variant calling.^{21–23} More precisely, the variants called by VarScan 2 were annotated by using the SeattleSeq Annotation 138 tool (<http://snpgs.washington.edu/SeattleSeqAnnotation138>) with the default setting. Variants annotated as SNPs according to dbSNP 138 (with the exception of *TP53* variants that were manually curated and scored as SNPs according to the International Agency for Research on Cancer *TP53* database; <http://p53.iarc.fr>), intronic variants mapping >2 bp before the start or after the end of coding exons, and synonymous variants were then filtered out. Among the remaining variants, only protein truncating variants (i.e. indels, stop codons and splice site mutations), as well as missense variants not included in the dbSNP 138 and annotated as somatic in the COSMIC v85 database (<https://cancer.sanger.ac.uk/cosmic>), were retained.

RNA-seq and ATAC-seq on primary CLL cells

Peripheral blood mononuclear cells from eight patients with *XPO1* mutations were sorted to purify the CLL CD19+/CD5+ tumoral cells and were subjected to RNAseq and ATACseq. Fifteen *XPO1* wild-type cases, matched for IGHV status, *TP53* status and FISH karyotype, were analysed for comparative purposes (Table S3). Further information is provided in the Supplementary Appendix.

Assessment of miR-155-5p expression

Cellular RNA was isolated by Trizol (Invitrogen) from 8 *XPO1* mutated CLL and from 8 *XPO1* wild type CLL matched for IGHV status, *TP53* status and FISH karyotype. The cDNA templates were prepared using the TaqMan Advanced miRNA cDNA Synthesis Kit (Applied Biosystems). RT-qPCR reactions were performed using the TaqMan Fast Advanced Master Mix (Applied Biosystems) with the miR-155-5p TaqMan Advanced MicroRNA Assay. The miR-186-5p was used as housekeeping gene. Experiments were carried out in duplicate. Quantitative miR expression data were acquired using the StepOnePlus Real-Time PCR system. The relative

miR-155-5p expression levels were determined using the comparative Ct ($2^{-\Delta\Delta Ct}$) method and the relative expression between the two groups was compared by the Wilcoxon rank sum exact test.

Statistical methods

The study endpoint was TTFT, defined as the time between presentation and start of first treatment of CLL because of progression to symptomatic disease according to the National Cancer Institute-Working Group/International Workshop on Chronic Lymphocytic Leukemia guidelines (patients without a documented event were censored at the date of last observation or death).^{10,24} Survival analysis was performed by the Kaplan–Meier method and compared between strata using the Log-rank test. The adjusted effects of *XPO1* mutations and the IPS-E¹⁸ and Rai 0 prognostic model¹⁹ variables on TTFT were estimated by Cox regression. The analysis was performed with the Statistical Package for the Social Sciences software v.24.0 (Chicago, IL).

RESULTS

Frequency of *XPO1* mutations in different phases of CLL

The prevalence of *XPO1* mutations was assessed across different clinical phases of CLL, including MBL ($n=95$), early-stage CLL ($n=957$), CLL relapsed after chemoimmunotherapy or pathway inhibitors ($n=81$), and CLL transformed into an aggressive lymphoma (Richter syndrome) ($n=55$). *XPO1* mutations occurred in 3.1% ($n=3/95$) of MBL, 2.9% ($n=28/957$) of early-stage CLL, 4.9% ($n=4/81$) of CLL relapsed after chemoimmunotherapy or pathway inhibitors and 12.7% (7/55) of CLL transformed into diffuse large B-cell lymphoma (Richter syndrome) (Figure S1A). The percentage of *XPO1* mutated patients was significantly higher in Richter syndrome when compared to MBL (12.7% vs. 3.1%, $p=0.03$) and early-stage CLL patients (12.7% vs. 2.9%, p value=0.002), respectively (Figure S1A).

Among Rai 0/I CLL provided with complete clinical and molecular data ($n=276$), after adjusting for multiple comparisons, *XPO1* mutations significantly correlated with an unmutated IGHV genes status and with a lymphocyte doubling time (LDT) <6 months ($p=0.02$; Figure S2).

Mutations of *XPO1* clustered in two hotspots. The first hotspot mapped at p.E571 accounted for 92.8% (39/42) of all mutations and affected a phylogenetically conserved position (Figure S1B). The glutamic acid in position 571 was commonly mutated into lysine or less frequently into glycine, alanine, or valine (Figure S1B). Mutations were selected to change the negatively charged glutamic acid of position 571 into a positively charged amino acid. The second hotspot mapped at p.D624 accounted for 7.1% (3/42) of mutations and appeared to be selectively restricted to CLL, while variants

affecting the p.E571 position have been described across different cancer types.⁵

To evaluate the potential clonal expansion of *XPO1* mutations during the CLL clinical course, we screened sequential samples of (i) CLL at the time of treatment requirement ($N=61$), (ii) CLL on ibrutinib treatment ($N=33$), and (iii) CLL transformed into Richter syndrome ($N=29$). The VAF of *XPO1* mutations remained stable over time (19.0% at the time of diagnosis vs. 27.0% at the time of treatment requirement, $p=0.206$) and no patient acquired *XPO1* mutations during the watch & wait period. Similarly, ibrutinib treatment did not associate with the emergence of *XPO1* mutations, as documented in 33 CLL cases followed at homogeneous time points every 24 weeks for at least 96 weeks.

Concerning *XPO1* mutation acquisition in Richter syndrome, 29 patients were analysed both in the CLL phase and in the lymph node biopsy affected by Richter syndrome.

XPO1 mutations were identified in 4 out of 29 cases of clonally related Richter syndrome. Three out of 4 cases displayed a mutation of *XPO1* in the Richter lymph node biopsy but not in the matched CLL phase, suggesting that *XPO1* mutations had been conceivably acquired at the time of Richter transformation.

XPO1 mutations impact on chromatin accessibility of CLL cells

To gain insights into the proliferative course of *XPO1*-mutated CLL, we searched for cellular programs associated with *XPO1* mutations. CLL cells were purified through flow-sorting from 8 patients harbouring *XPO1* mutations (VAF from 25% to 50%) and from 15 patients lacking *XPO1* mutations used as controls. *XPO1* mutated and *XPO1* wild-type

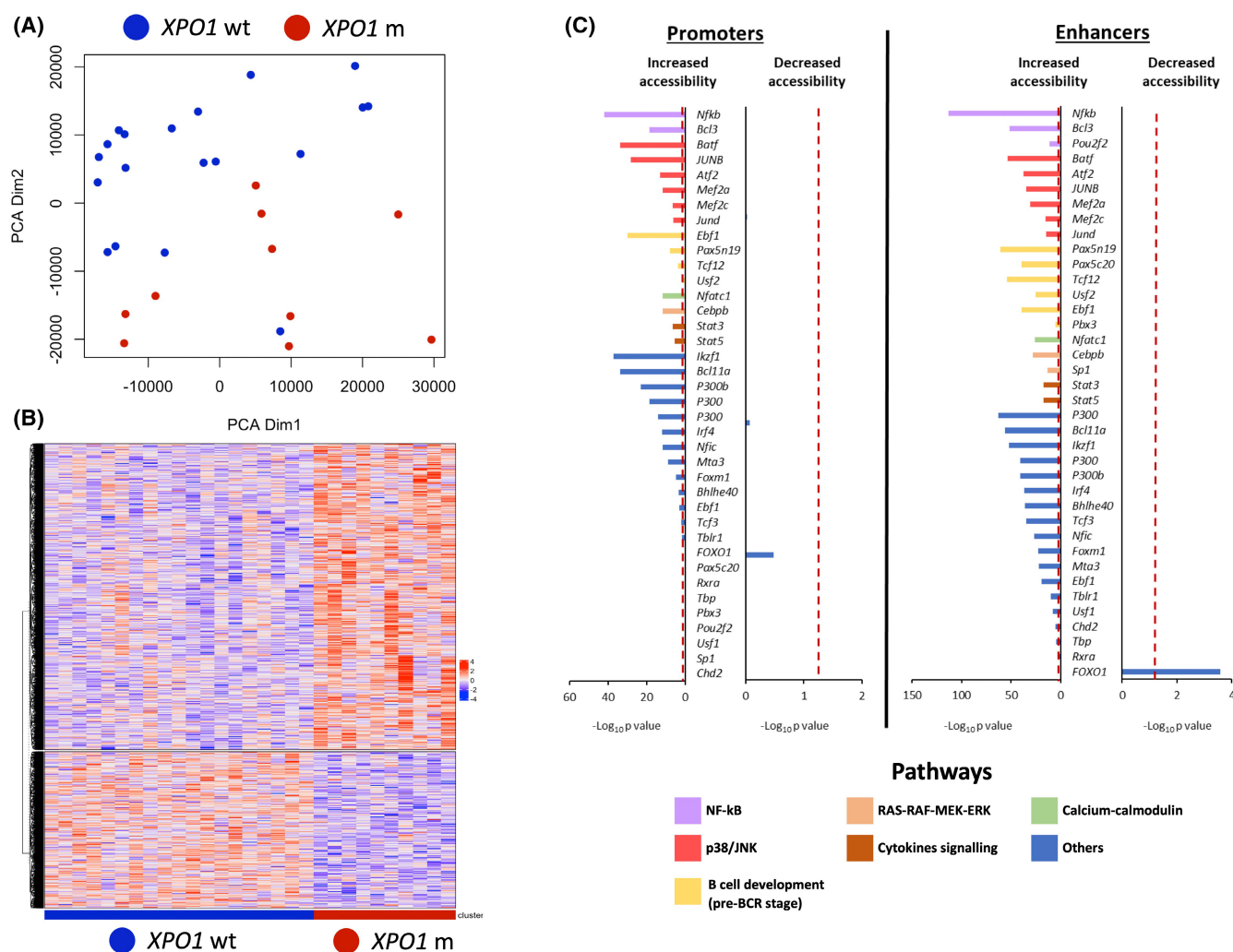


FIGURE 1 Different chromatin accessibility in *XPO1* mutated compared to wild-type chronic lymphocytic leukaemia (CLL). (A) Multidimensional scaling (MDS) plot of the diverse chromatin accessibility between *XPO1* mutant (in red) and *XPO1* wild type cases (in blue) demonstrates distinct clustering between mutated and non-mutated CLL samples along MDS dimension. (B) Heatmap of signal intensity shows the different chromatin accessibility in *XPO1* mutant and in *XPO1* wild type CLL. (C) Bar plots showing gene promoter and/or enhancer regions that present a significantly different chromatin accessibility in *XPO1* mutated CLL. The dot red lines denote statistical significance. The bars are colour-coded according to signalling pathways reported in the legend below the graph.

CLL samples were matched for the main biological CLL characteristics (IGHV, *TP53* status and FISH karyotype) to mitigate biases related to the disease genetic background. Samples were profiled for both chromatin accessibility and transcriptome.

By principal component analysis (PCA), *XPO1* mutated CLL clearly separated and showed a distinct chromatin profile compared to wild-type cases ($p=0.00356$) (Figure 1A). Overall, *XPO1* mutated CLL had a chromatin landscape more accessible than that of *XPO1* wild type CLL, with 6391 enhancers/promoters being more accessible and only 3283 enhancers/promoters being less accessible in *XPO1* mutated compared to *XPO1* wild type (FDR < 0.1).

Differentially accessible chromatin regions were decorated with the CLL-specific map of enhancers and active promoters, and with the map of 96 transcription factor binding sites of B cells²⁵ (Figure 1B). Chromatin regions that were more accessible in *XPO1* mutated CLL were enriched in binding sites for transcription factors that are downstream the pathways emanating from the BCR, including NF- κ B signalling (NF- κ B, BCL3 and OCT2), p38-JNK (JUNB, JUND, MEF2A, MEF2C and ATF2), RAS-RAF-MEK-ERK (CEBPB, SP1) and calcium-calmodulin (NFATC1). Chromatin regions

that were more accessible in *XPO1* mutated CLL were also enriched in binding sites for transcription factors that are regulated by the cytokine/inflammation signalling (STAT3 and STAT5) (Figure 1C). Chromatin regions that were less accessible in *XPO1* mutated CLL were enriched in binding sites of FOXO1, whose nuclear localization is blocked by active BCR signalling.

The transcriptome of *XPO1* mutated CLL cells is enriched in MAPK and inflammation signalling genes

Overall, 236 genes were upregulated, and 296 genes were downregulated in *XPO1* mutant CLL compared to *XPO1* wild-type CLL. Consistently, by PCA, *XPO1* mutated cases showed a distinct transcriptomic profile compared to *XPO1* wild-type cases ($p=0.0126$; Figure 2A,B). In keeping with the chromatin accessibility changes observed by ATAC-seq, *XPO1* mutated CLL cells showed several transcriptomic features associated with BCR and cytokine signalling. Among pathways enriched in the upregulated genes, these included immediate early response to BCR activation, TGF β

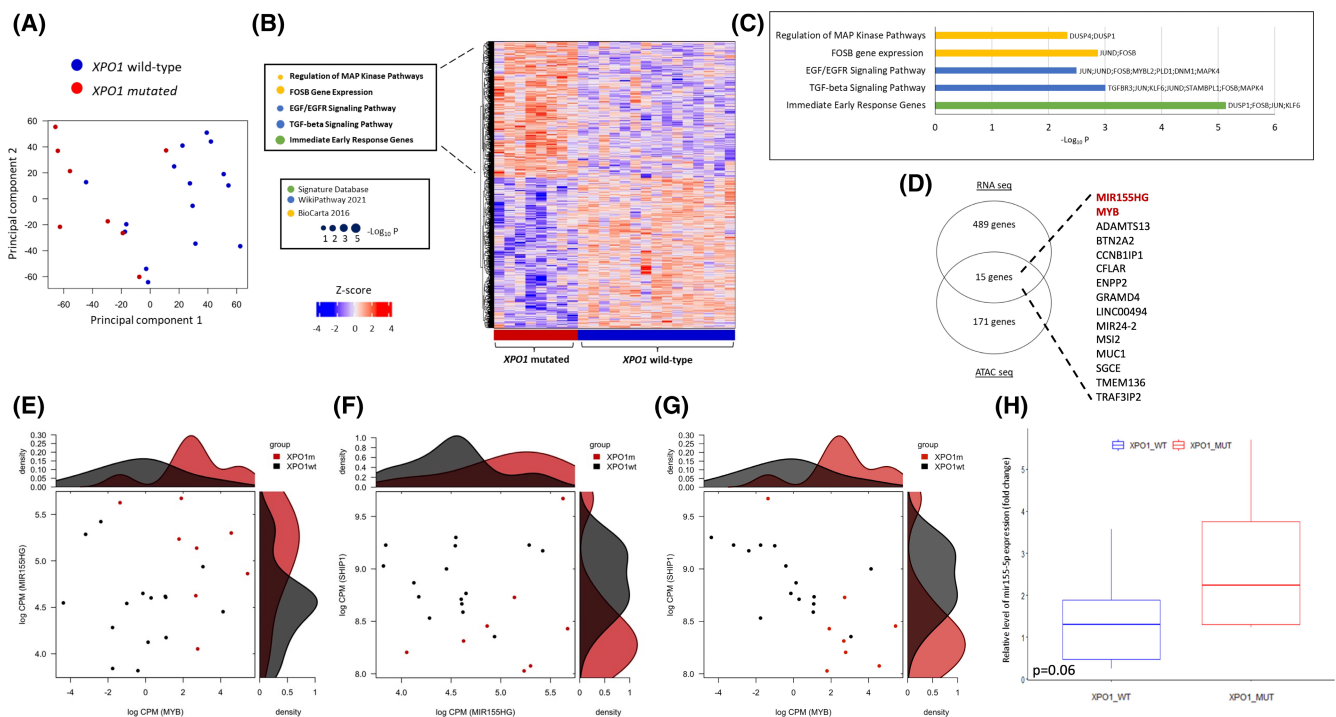


FIGURE 2 Different gene expression profile in *XPO1* mutated compared to wild-type chronic lymphocytic leukaemia (CLL). (A) Multidimensional scaling (MDS) plot of the diverse chromatin accessibility between *XPO1* mutant (in red) and *XPO1* wild type cases (in blue) demonstrates distinct clustering between mutated and non-mutated CLL samples along MDS dimension. (B) Heatmap demonstrating differential expression of genes between *XPO1* mutant (in red) and *XPO1* wild type (in blue) CLL. The left side of the heatmap represents the gene ontology analysis for biological processes significantly enriched in *XPO1* mutated CLL. (C) The histogram represents the pathway enrichment analysis of the upregulated genes in *XPO1* mutant CLL. (D) Venn diagrams representing the number of genes upregulated by RNA-seq and whose promoters are more accessible by ATAC-seq in *XPO1* mutated CLL. The intersection between the diagrams represents the 15 genes that are upregulated and whose promoter is more accessible. The density plots represented in panels (E–G) denote the association of *MIR155HG*, *MYB* and *SHIP1* in *XPO1* mutated (in red) and in *XPO1* wild type (in grey) CLL cells. (H) The box plot denotes the relative expression of target miR-155-5p compared to endogenous control (miR-186-5p) in *XPO1* mutated (in red) and *XPO1* wild-type cells (in blue).

signalling, EGF-EGFR signalling, FOSB gene expression and regulation of MAPK through DUSP (Figure 2C). The DUSP1 nuclear phosphatase, that inhibits JUN/FOS signalling, was upregulated in *XPO1* mutant CLL and represents a potential candidate as cargo protein for *XPO1*. Using the Wregex prediction tool,²⁶ we identified two different NES in DUSP1. Both NES show a negative charge in the amino-acid C-terminal residues (Table S4), suggesting that DUSP1 could better interact with *XPO1*^{E571K} mutations.

The ATAC-seq and RNA-seq profiles of *XPO1* mutant CLL identify upregulation of the *miR-155/MYB* pathway

By combining transcriptomic and epigenomic data, we identified 15 genes that are upregulated by RNA-seq and whose promoters are more accessible by ATAC-seq (Figure 2D). These genes include *MIR155HG*, the host gene that generates miR-155, and *MYB*, a transcription factor that positively regulates miR-155 expression. Given their role in BCR signalling, *MIR155HG* and *MYB* were further investigated.²⁷ As expected, higher levels of *MIR155HG* correlated with higher levels of *MYB* in *XPO1* mutant CLL ($p < 0.05$; Figure 2E). miR-155 expression favours BCR signalling through several mechanisms, including the downmodulation of SHIP1,²⁸ a phosphatase that inhibits the BCR cascade. Accordingly, an inverse correlation between *MIR155HG* and *MYB* levels with SHIP1 levels was observed in *XPO1* mutant CLL (all $p < 0.05$; Figure 2F,G).

To confirm that a higher expression of *MIR155HG* correlates with higher miR-155 levels, we measured miR-155 by RT-qPCR in *XPO1* mutated ($n = 8$) and wild type ($n = 8$) CLL matched for IGHV status and FISH karyotype. Quantitative analysis confirmed the higher expression of *miR-155* in *XPO1* mutated CLL compared to *XPO1* wild-type CLL ($p = 0.065$; Figure 2H). In addition, the *SPI1/PU.1* gene, a transcription factor that is inhibited by *miR-155*,²⁹ was found to be significantly downregulated in *XPO1* mutated cases ($p = 0.0029$), thus cross-validating the *miR-155* overexpression in *XPO1* mutated CLL.

Association between *XPO1* mutations and TTFT

As *XPO1* mutated CLL were marked by the BCR and proliferation programs, we asked if *XPO1* mutated CLL patients are characterized by a more aggressive clinical course. A retrospective, training validation design was used for the analysis in three different independent cohorts. To purify the impact of *XPO1* mutations on clinical proliferation of CLL, only early-stage patients initially managed with a watch-and-wait policy were considered. *XPO1* was mutated in 8/276 (2.9%) patients of the 1st cohort, in 12/286 (4.2%) patients in the 2nd cohort and in 8/395 (2.0%) patients in the 3rd cohort. The complete clinical and biological profile of the three cohorts is reported in Table 1. As expected for

TABLE 1 Patients' characteristics.

Characteristics	1st cohort Values	2nd cohort Values	3rd cohort Values
Median age	70.9 (62.1–76.9)	67.0 (56.0–73.0)	>65 years 55.0%
Median lymphocytes/ μ L	8250	4151	NA
B2M mg/L	2.1 (1.7–2.6)	NA	NA
Gender			
Male	143 (51.8%)	125 (57.8%)	NA
Female	133 (48.2%)	91 (42.1%)	NA
13q deletion			
Yes	141 (51.1%)	NA	NA
No	131 (47.5%)	NA	NA
Trisomy 12			
Yes	41 (14.9%)	35 (12.2%)	56 (14.2%)
No	231 (83.7%)	217 (75.9%)	339 (85.8%)
11q deletion			
Yes	14 (5.1%)	NA	34 (8.6%)
No	258 (93.5%)	NA	361 (91.4%)
17p deletion			
Yes	10 (3.6%)	10 (3.5%)	25 (6.3%)
No	262 (94.9%)	344 (85.3%)	370 (93.7%)
IGHV mutational status			
Mutated	198 (71.7%)	173 (60.5%)	291 (74.0%)
Unmutated	68 (24.6%)	112 (39.2%)	102 (26.0%)

Abbreviations: B2M, beta-2-microglobulin; IGHV, immunoglobulin heavy chain variable.

patients with early-stage CLL, high-risk molecular features were rare.

After a median follow-up of 10.4 years, *XPO1* mutations were significantly associated with a shorter TTFT in the 1st cohort, with a TTFT at 10 years of 0% in *XPO1* mutated patients compared to 69.8% in wild-type cases (Figure 3A) (HR 9.8, 95% CI 4.35–22.14, $p < 0.001$). In multivariate analysis including the IPS-E variables,¹⁸ which are validated for predicting TTFT and include unmutated IGHV genes, palpable lymph nodes and lymphocyte count $>15000/\mu$ L, *XPO1* mutations maintained an independent association with a shorter TTFT (HR 2.79, 95% CI 1.16–6.71, $p = 0.022$; Table 2). *XPO1* mutations maintained an independent association with a shorter TTFT (HR 3.56, 95% CI 1.48–8.59, $p = 0.005$) also after adjusting for variables of the Rai 0 prognostic score (Table 3)¹⁹ and *NOTCH1* and *SF3B1* mutations (Table S5). In the other two cohorts, *XPO1* mutations were confirmed as a prognosticator of shorter TTFT. In the 2nd cohort, after a median follow-up of 5.6 years, the TTFT at 6 years was 25.0% in *XPO1* mutated cases compared to 61.3% in *XPO1* wild type cases ($p = 0.025$; HR 2.24, 95% CI 1.09–4.61, $p = 0.029$; Figure 3B). In the 3rd cohort, after a median follow-up of 6.7 years, the TTFT at 7 years was 0% in *XPO1* mutated patients compared to 73.4% in wild-type patients ($p < 0.0001$; HR 6.02, 95% CI 2.48–15.03, $p < 0.001$; Figure 3C).

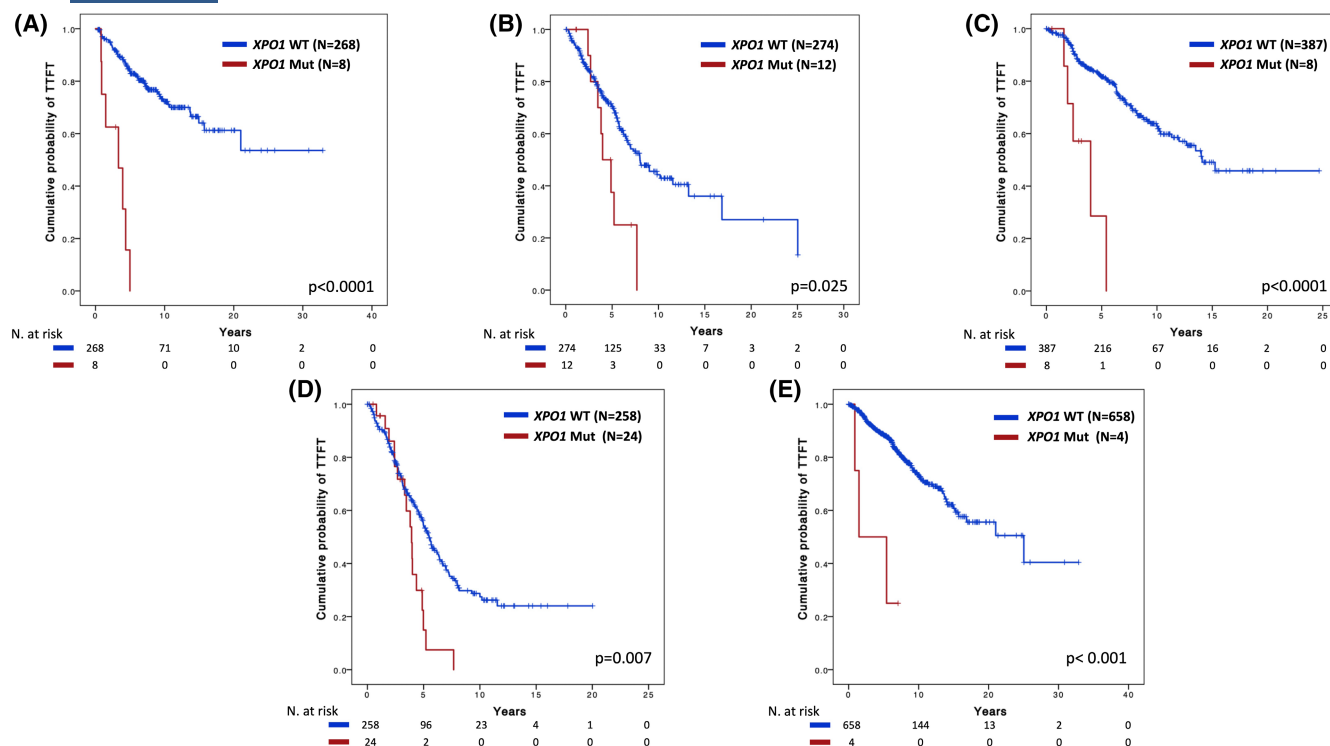


FIGURE 3 Prognostic impact of *XPO1* mutations. Kaplan–Meier estimates of time to first treatment in the 1st cohort of 276 Rai 0/I chronic lymphocytic leukaemia (CLL) (A), in the 2nd cohort of 286 Binet A CLL (B), and in the 3rd cohort of 395 Rai 0 CLL (C). Cases harbouring *XPO1* mutations are represented by the red line and wild type cases are represented by the blue line. Panel (D and E) represent the clinical impact of *XPO1* mutations in immunoglobulin heavy chain variable (IGHV) unmutated and IGHV mutated patients, respectively. Cases harbouring *XPO1* mutations are represented by the red line and wild type cases are represented by the blue line. The log-rank statistics *p* values are indicated adjacent to the curves.

TABLE 2 Multivariate analysis for *XPO1* mutations and IPS-E variables.

Variable	HR	95% CI	<i>p</i> value
Unmutated IGHV	3.60	2.18–5.96	<0.0001
Palpable lymph nodes	2.71	1.63–4.70	<0.001
Lymphocyte >15000/ μ L	2.49	1.50–4.11	<0.001
<i>XPO1</i> mutations	2.79	1.16–6.71	0.022

Abbreviations: CI, confidence interval; HR, hazard ratio; IGHV, immunoglobulin heavy chain variable.

By combining all cohorts ($N=957$ patients), patients carrying either *XPO1* E571 ($N=25$) or D624 ($N=3$) mutations showed superimposable outcomes in terms of TTFT ($p=0.594$; Figure S3). In addition, the prognostic value of *XPO1* mutations in terms of shorter TTFT was maintained in patients with both mutated and unmutated IGHV genes (Figure 3D,E).

The IPS-E and Rai 0 models provide a benchmark of the expected TTFT in patients with high-risk early-stage CLL. We sought to understand whether early-stage CLL with *XPO1* mutations has a similarly poor TTFT as early-stage CLL defined as high-risk by the IPS-E and Rai 0 models. The TTFT of early-stage patients harbouring *XPO1* mutations, irrespective of their IPS-E score, did not significantly differ from the TTFT of early-stage patients belonging to the high-risk class

TABLE 3 Multivariate analysis for *XPO1* mutations and Rai 0 prognostic score variables.

Variable	HR	95% CI	<i>p</i> value
WBC > 32000/ μ L	2.73	1.08–6.38	0.033
Unmutated IGHV	4.00	2.37–6.76	<0.0001
Del 17p	1.63	0.49–5.42	0.493
Tris 12	1.68	0.89–3.13	0.104
Del 11q	0.78	0.28–2.20	0.641
<i>XPO1</i> mutations	3.56	1.48–8.59	0.005

Abbreviations: CI, confidence interval; HR, hazard ratio; IGHV, immunoglobulin heavy chain variable; WBC, white blood cells.

according to IPS-E (Figure 4A). Similarly, the TTFT of early-stage patients harbouring *XPO1* mutations, irrespective of their Rai 0 score, did not significantly differ from the TTFT of early-stage patients belonging to the high-risk class according to the Rai 0 model (Figure 4B). *XPO1* mutations therefore identify patients with early treatment requirements independent of IPS-E and Rai 0 prognostic models.

DISCUSSION

Most CLL patients are diagnosed in an asymptomatic stage and are managed with a watch-and-wait strategy.¹⁰ However,

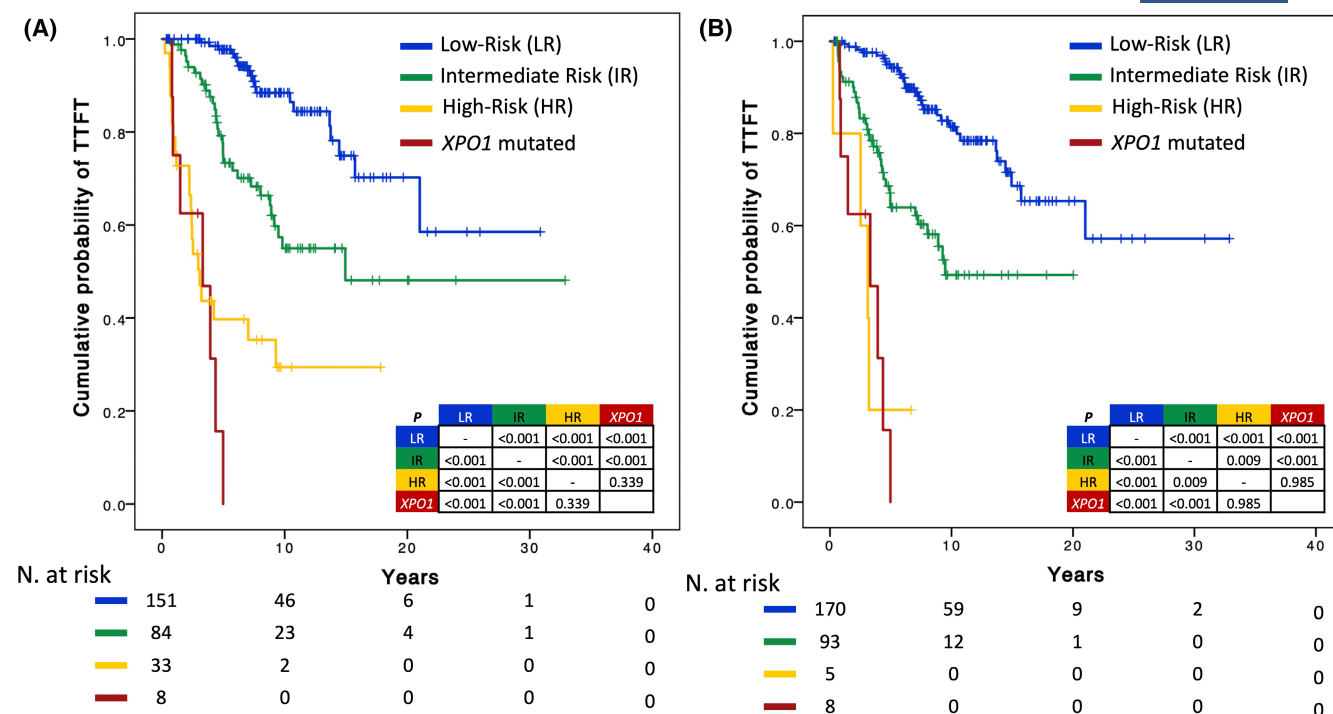


FIGURE 4 Prognostic impact of *XPO1* mutations integrated into prognostic scores for early stage chronic lymphocytic leukaemia (CLL). (A) Kaplan–Meier estimates of time to first treatment (TTFT) in 276 Rai 0/I CLL according to the IPS-E and *XPO1* mutations. Low-risk patients are represented by the blue line, intermediate-risk patients by the green line, high risk patients by the yellow line and *XPO1* mutated patients by the red line. (B) Kaplan–Meier estimates of TTFT in 276 Rai 0 and I CLL according to the Rai 0 prognostic score and *XPO1* mutations. Low-risk patients are represented by the blue line, intermediate-risk patients by the green line, high risk patients by the yellow line and *XPO1* mutated patients by the red line. The pairwise log-rank statistics *p* values are indicated in the tables adjacent to the curves.

their clinical outcome is heterogeneous and different patients may progress and require therapy at different timepoints. In the present study using a training-validation approach, *XPO1* mutations emerged as an independent predictor of shorter TTFT capturing a fraction of patients that require treatment soon after diagnosis. *XPO1* mutant CLL cells are characterized by a higher expression of signalling pathways downstream to the BCR that may predispose to a higher proliferative behaviour.

To gain insights into the mechanisms that may drive the shorter TTFT and LDT of *XPO1* mutated CLL, we evaluated the transcriptomic and the epigenomic profile of *XPO1* mutated CLL and compared it to that of wild type cases matched for IGHV status, FISH karyotype and *TP53* status. BCR signalling appeared as a potential candidate that might contribute, at least in part, to the higher proliferation rate of *XPO1*-mutated CLL. In fact, chromatin regions that were more accessible in *XPO1* mutated CLL were enriched in binding sites for transcription factors that act downstream to pathways emanating from the BCR. These pathways include NF- κ B signalling, p38-JNK, RAS-RAF-MEK-ERK and calcium-calmodulin. In addition, the combination of RNA-seq and ATAC-seq data identified the overexpression and the increased promoter accessibility of the *MYB* and *MIR155HG* genes in *XPO1* mutated CLL compared to wild-type cases. Importantly, *MYB* is known to induce expression of *MIR155HG*, the gene coding for miR-155 that inhibits the expression of SHIP-1 and, consequently, contributes to

stimulate the activity of the BCR. These results provide novel evidence in primary CLL cells on the association between *XPO1* mutation and an enrichment in pathways regulating lymphocyte activation, NFAT signalling and NF- κ B activation. Also, these data integrate and expand previous suggestions on the association of *XPO1* mutations with genes of the inflammation and cytokine signalling pathways.^{5,30}

The precise mechanisms by which *XPO1* mutations induce the upregulation of *miR-155* and of other signalling pathways remain currently unknown. In our study, *DUSP1*, encoding a nuclear phosphatase that inhibits JUN/FOS signalling, has been identified by RNA-seq as one of the major upregulated genes in *XPO1* mutant CLL patients. The WregeX prediction model generated in our study has identified two different negatively charged NES domains in the *DUSP1* protein, rendering it a candidate of increased export out of the nucleus in the presence of *XPO1* mutations that enhance export of proteins bearing a negative NES domain. Nuclear export of *DUSP1* may in turn favour JUN/FOS signalling in the nucleus. Since the *MIR155HG* promoter contains a conserved binding site for JUN/FOS,³¹ an enhanced signalling of this pathway could promote the transcription of *MIR155HG*, that would promote BCR signalling through miR-155. In vitro, studies will be required to confirm the hypothesis generated by our current data.

Since the transcriptomic and epigenomic profile of *XPO1* mutated CLL pointed to pathways that promote BCR signalling and may affect CLL proliferation, we analysed

the correlation of *XPO1* mutations with TTFT. Previous reports demonstrated conflicting results regarding the prognostic impact of *XPO1* mutations as a marker for shorter TTFT conceivably because they included CLL patients at different clinical stages.^{20,30,32} In this study, by including only early-stage CLL (Rai 0/I and Binet A), *XPO1* mutations were sorted out as a validated prognosticator of shorter TTFT. Importantly, the prognostic role of *XPO1* mutations in anticipating TTFT in early-stage CLL is independent of the IGHV status and of the variables included in the two prognostic scores for early-stage CLL patients.^{18,19} Since two unique codons are the hotspots affected by *XPO1* mutations in CLL, primer-based methods may be used to identify *XPO1* mutations in a simple and time effective manner. Prediction of TTFT may be important to identify high-risk patients that might be suitable for early intervention clinical trials and to reassure patients with a very indolent disease that may be followed with a less intense schedule.^{18,19}

Finally, the longitudinal analysis of CLL samples harbouring *XPO1* mutations showed that the *XPO1* mutant clone did not undergo clonal expansion either during watch & wait management or after therapy, including chemoimmunotherapy and ibrutinib. This observation may suggest that *XPO1* mutations are not selected by treatment. Conversely, the acquisition of *XPO1* mutations was observed in the lymph node biopsy of patients who transformed to clonally related Richter syndrome, suggesting that *XPO1* mutations might represent a novel mechanism involved in Richter transformation.

AUTHOR CONTRIBUTIONS

Gianluca Gaidano, Davide Rossi and Riccardo Moia designed the study, interpreted data, and wrote the manuscript; Valter Gattei and Robin Foà contributed to study design and manuscript revision; Lodovico di Terzi Bergamo, Donatella Talotta, Riccardo Bomben, Gabriela Forestieri, Valeria Spina, Alessio Bruscaggini, Tamara Bittolo and Antonella Zucchetto performed molecular studies and contributed to manuscript revision; Chiara Cosentino, Mohammad Almasri, Riccardo Dondolin, Silvia Rasi, Abdurraouf Mahmoud, Wael Al Essa, Bassel Awikeh, Sreekar Kogila, Matteo Bellia and Samir Mouhssine contributed to data analysis and manuscript preparation; Stefano Baldoni, Ilaria Del Giudice, Francesca Romana Mauro, Rossana Maffei, Annalisa Chiarenza, Agostino Tafuri, Roberta Laureana, Maria Ilaria Del Principe, Francesco Zaja, Giovanni D'Arena, Jacopo Olivieri, Paolo Sportoletti, Roberto Marasca, Lydia Scarfò and Paolo Ghia provided study material and contributed to manuscript revision.

ACKNOWLEDGEMENTS

This work was supported by: Molecular bases of disease dissemination in lymphoid malignancies to optimize curative therapeutic strategies, (5 × 1000 No. 21198), Associazione Italiana per la Ricerca sul Cancro Foundation Milan, Italy; Progetti di Rilevante Interesse Nazionale

(PRIN; 2015ZMRFEA), Rome, Italy; the AGING Project—Department of Excellence—DIMET, Università del Piemonte Orientale, Novara, Italy; and Ricerca Finalizzata 2018 (project RF-2018-12365790), MoH, Rome, Italy; Swiss Cancer League, ID 3746, 4395 4660, and 4705, Bern, Switzerland; Research Advisory Board of the Ente Ospedaliero Cantonale, ABREOC 2019-22514, Bellinzona, Switzerland; European Research Council (ERC) Consolidator Grant CLLCLONE, ID: 772051; Swiss National Science Foundation, ID 320030_169670/1 and 310030_192439, Berne, Switzerland; Fondazione Fidinam, Lugano, Switzerland; Nelia & Amadeo Barletta Foundation, Lausanne, Switzerland; Fond'Action, Lausanne, Switzerland; The Leukemia & Lymphoma Society, Translational Research Program, ID 6594-20, New York. The authors are grateful to Ahad Ahmed Kodipad and Chiara Favini for their technical help with this study.

CONFLICT OF INTEREST STATEMENT

The authors have no conflict of interests regarding this manuscript.

DATA AVAILABILITY STATEMENT

The data that support the findings of this study are available from the corresponding author upon reasonable request.

ORCID

Riccardo Moia  <https://orcid.org/0000-0001-7393-1138>
 Riccardo Bomben  <https://orcid.org/0000-0002-8746-9404>
 Ilaria Del Giudice  <https://orcid.org/0000-0001-6864-9533>
 Francesca Romana Mauro  <https://orcid.org/0000-0003-2425-9474>
 Rossana Maffei  <https://orcid.org/0000-0002-3518-2006>
 Giovanni D'Arena  <https://orcid.org/0000-0002-3807-7287>
 Paolo Sportoletti  <https://orcid.org/0000-0002-5630-9862>
 Lydia Scarfò  <https://orcid.org/0000-0002-0844-0989>
 Paolo Ghia  <https://orcid.org/0000-0003-3750-7342>
 Robin Foà  <https://orcid.org/0000-0002-5021-3026>
 Gianluca Gaidano  <https://orcid.org/0000-0002-4681-0151>

REFERENCES

- Landau DA, Tausch E, Taylor-Weiner AN, Stewart C, Reiter JG, Bahlo J, et al. Mutations driving CLL and their evolution in progression and relapse. *Nature*. 2015;526(7574):525–30.
- Puente XS, Beà S, Valdés-Mas R, Villamor N, Gutiérrez-Abril J, Martín-Subero JL, et al. Non-coding recurrent mutations in chronic lymphocytic leukaemia. *Nature*. 2015;526(7574):519–24.
- Knisbacher BA, Lin Z, Hahn CK, Nadeu F, Duran-Ferrer M, Stevenson KE, et al. Molecular map of chronic lymphocytic leukemia and its impact on outcome. *Nat Genet*. 2022;54(11):1664–74.
- Azmi AS, Uddin MH, Mohammad RM. The nuclear export protein XPO1—from biology to targeted therapy. *Nat Rev Clin Oncol*. 2021;18(3):152–69.
- Taylor J, Sendino M, Gorelick AN, Pastore A, Chang MT, Penson AV, et al. Altered nuclear export signal recognition as a driver of oncogenesis. *Cancer Discov*. 2019;9(10):1452–67.
- Burger JA, Chiorazzi N. B cell receptor signaling in chronic lymphocytic leukemia. *Trends Immunol*. 2013;34(12):592–601.
- Stevenson FK, Krysov S, Davies AJ, Steele AJ, Packham G. B-cell receptor signaling in chronic lymphocytic leukemia. *Blood*. 2011;118(16):4313–20.

8. Dühren-von Minden M, Übelhart R, Schneider D, Wossning T, Bach MP, Buchner M, et al. Chronic lymphocytic leukaemia is driven by antigen-independent cell-autonomous signalling. *Nature*. 2012;489(7415):309–12.
9. Minici C, Gounari M, Übelhart R, Scarfò L, Dühren-von Minden M, Schneider D, et al. Distinct homotypic B-cell receptor interactions shape the outcome of chronic lymphocytic leukaemia. *Nat Commun*. 2017;8:15746.
10. Hallek M, Cheson BD, Catovsky D, Caligaris-Cappio F, Dighiero G, Döhner H, et al. iwCLL guidelines for diagnosis, indications for treatment, response assessment, and supportive management of CLL. *Blood*. 2018;131(25):2745–60.
11. Dighiero G, Maloum K, Desablens B, Cazin B, Navarro M, Leblay R, et al. Chlorambucil in indolent chronic lymphocytic leukemia. French Cooperative Group on Chronic Lymphocytic Leukemia. *N Engl J Med*. 1998;338(21):1506–14.
12. Herling CD, Cymbalista F, Groß-Ophoff-Müller C, Bahlo J, Robrecht S, Langerbeins P, et al. Early treatment with FCR versus watch and wait in patients with stage Binet A high-risk chronic lymphocytic leukemia (CLL): a randomized phase 3 trial. *Leukemia*. 2020;34(8):2038–50.
13. Hoehstetter MA, Busch R, Eichhorst B, Bühler A, Winkler D, Eckart MJ, et al. Early, risk-adapted treatment with fludarabine in Binet stage A chronic lymphocytic leukemia patients: results of the CLL1 trial of the German CLL study group. *Leukemia*. 2017;31(12):2833–7.
14. Langerbeins P, Zhang C, Robrecht S, Cramer P, Fürstenau M, Al-Sawaf O, et al. The CLL12 trial: ibrutinib vs placebo in treatment-naïve, early-stage chronic lymphocytic leukemia. *Blood*. 2022;139(2):177–87.
15. Gruber M, Bozic I, Leshchiner I, Livitz D, Stevenson K, Rassenti L, et al. Growth dynamics in naturally progressing chronic lymphocytic leukaemia. *Nature*. 2019;570(7762):474–9.
16. Moia R, Patriarca A, Deambrogi C, Rasi S, Favini C, Kodipad AA, et al. An update on: molecular genetics of high-risk chronic lymphocytic leukemia. *Expert Rev Hematol*. 2020;13(2):109–16.
17. Baumann T, Moia R, Gaidano G, Delgado J, Condoluci A, Villamor N, et al. Lymphocyte doubling time in chronic lymphocytic leukemia modern era: a real-life study in 848 unselected patients. *Leukemia*. 2021;35(8):2325–31.
18. Condoluci A, Terzi di Bergamo L, Langerbeins P, Hoehstetter MA, Herling CD, De Paoli L, et al. International prognostic score for asymptomatic early-stage chronic lymphocytic leukemia. *Blood*. 2020;135(21):1859–69.
19. Cohen JA, Rossi FM, Zucchetto A, Bomben R, Terzi-di-Bergamo L, Rabe KG, et al. A laboratory-based scoring system predicts early treatment in Rai 0 chronic lymphocytic leukemia. *Haematologica*. 2020;105(6):1613–20.
20. Mansouri L, Thorvaldsdottir B, Sutton LA, Karakatsoulis G, Meggendorfer M, Parker H, et al. Different prognostic impact of recurrent gene mutations in chronic lymphocytic leukemia depending on IGHV gene somatic hypermutation status: a study by ERIC in HARMONY. *Leukemia*. 2023;37(2):339–47.
21. Diop F, Moia R, Favini C, Spaccarotella E, De Paoli L, Bruscaggin A, et al. Biological and clinical implications of BIRC3 mutations in chronic lymphocytic leukemia. *Haematologica*. 2020;105(2):448–56.
22. Moia R, Favini C, Ferri V, Forestieri G, Terzi Di Bergamo L, Schipani M, et al. Multiregional sequencing and circulating tumour DNA analysis provide complementary approaches for comprehensive disease profiling of small lymphocytic lymphoma. *Br J Haematol*. 2021;195(1):108–12.
23. Bomben R, Rossi FM, Vit F, Bittolo T, D'Agaro T, Zucchetto A, et al. TP53 mutations with low variant allele frequency predict short survival in chronic lymphocytic leukemia. *Clin Cancer Res*. 2021;27(20):5566–75.
24. Cheson BD, Bennett JM, Grever M, Kay N, Keating MJ, O'Brien S, et al. National Cancer Institute-sponsored Working Group guidelines for chronic lymphocytic leukemia: revised guidelines for diagnosis and treatment. *Blood*. 1996;87(12):4990–7.
25. Beekman R, Chapaprieta V, Russiñol N, Vilarrasa-Blasi R, Verdaguer-Dot N, Martens JHA, et al. The reference epigenome and regulatory chromatin landscape of chronic lymphocytic leukemia. *Nat Med*. 2018;24(6):868–80.
26. Prieto G, Fullaondo A, Rodriguez JA. Prediction of nuclear export signals using weighted regular expressions (Wregex). *Bioinformatics*. 2014;30(9):1220–7.
27. Cui B, Chen L, Zhang S, Mraz M, Fecteau JF, Yu J, et al. MicroRNA-155 influences B-cell receptor signaling and associates with aggressive disease in chronic lymphocytic leukemia. *Blood*. 2014;124(4):546–54.
28. Mraz M, Kipps TJ. MicroRNAs and B cell receptor signaling in chronic lymphocytic leukemia. *Leuk Lymphoma*. 2013;54(8):1836–9.
29. Lu D, Nakagawa R, Lazzaro S, Staudacher P, Abreu-Goodger C, Henley T, et al. The miR-155-PU.1 axis acts on Pax5 to enable efficient terminal B cell differentiation. *J Exp Med*. 2014;211(11):2183–98.
30. Walker JS, Hing ZA, Harrington B, Baumhardt J, Ozer HG, Lehman A, et al. Recurrent XPO1 mutations alter pathogenesis of chronic lymphocytic leukemia. *J Hematol Oncol*. 2021;14(1):17.
31. Yin Q, Wang X, McBride J, Fewell C, Flemington E. B-cell receptor activation induces BIC/miR-155 expression through a conserved AP-1 element. *J Biol Chem*. 2008;283(5):2654–62.
32. Hu B, Patel KP, Chen HC, Wang X, Luthra R, Routhort MJ, et al. Association of gene mutations with time-to-first treatment in 384 treatment-naïve chronic lymphocytic leukaemia patients. *Br J Haematol*. 2019;187(3):307–18.

SUPPORTING INFORMATION

Additional supporting information can be found online in the Supporting Information section at the end of this article.

How to cite this article: Moia R, Terzi di Bergamo L, Talotta D, Bomben R, Forestieri G, Spina V, et al. *XPO1* mutations identify early-stage CLL characterized by shorter time to first treatment and enhanced BCR signalling. *Br J Haematol*. 2023;203(3):416–425. <https://doi.org/10.1111/bjh.19052>